



## On the use of atmospheric instability indices based on NWP model production for thunderstorm forecast

**Boryana Tsenova, Andrey Bogatchev**

*National Institute of Meteorology and Hydrology,  
Tsarigradsko shose 66, 1784 Sofia, Bulgaria*

(Received: 23 Jul 2020, Accepted: 09 Oct 2020)

**Abstract:** The atmospheric instability over Bulgaria assessed based on ALADIN-BG forecast production for the warm half-year of 2018 and 2019 is evaluated and connected to the detected lightning. Lightning data are taken from ATDnet. Four instability indices, calculated based on forecasted thermodynamical fields in the atmosphere, showed a relatively good ability to discriminate thunderstorm cases from the non thunderstorm ones, depending on the month and could be considered for predicting thunderstorm probability formation over different regions. However, they should not be used as a sole tool for a more accurate thunderstorm forecast.

**Keywords:** Thunderstorm, lightning, instability indices, NWP model, ALADIN-BG

---

### 1. INTRODUCTION

The study of atmospheric electricity and especially lightning is developing rapidly as technology advances. The evaluation of lightning electric and magnetic field is important as because of their fundamental importance, as well for its more precise forecast. Thunderstorms are dangerous phenomena and their accurate in terms of time and location forecast is necessary. Due to the established relationships between the nature of lightning and other dangerous natural phenomena such as tornadoes, torrential rains, floods, hail storms, destructive winds and forest fires, a better understanding of lightning behavior could improve the nowcasting of some hazards by a timely accurate numerical forecast of thunderstorm development probability.

Atmospheric instability is a critical factor in the development of severe weather, and severe weather instability indices can be a useful tool when applied correctly to a

given convective weather situation. Atmospheric instability indices show the potential for convection developing in the atmosphere. Many thermodynamic parameters and derived indices, particularly those from vertical sounding using radiosondes, are used as diagnostic variables or precursors of thunderstorms and heavy rainfall, such as Lifted Index (LI) (Galway, 1956), K Index (KI) (George, 1960), Totals Total Index (TT) (Miller, 1972) and many others. More complex indices have been elaborated from these basic indices for other specific purposes. Such indices simplify the task of analyzing and assessing the complex three-dimensional structure of the atmosphere and as such are a very beneficial tool for operational forecasters who usually have to work under prescribed deadlines (Doswell and Schultz, 2006). Threshold values for the different indices were determined for the forecast of severe weather. However they vary with the geographic location. For Bulgaria, several studies on different instability indices were performed based on vertical sounding data (Tsenova and Kolev, 2008), and based on both sounding and model data (Tsenova and Bogatchev, 2012; Markova, 2013; Markova et al., 2015). Due to the temporal and spatial restrictions of radiosondes measurements, with the rapid development and improvement of the numerical weather prediction (NWP) models, models are increasingly used in practice to forecast the atmospheric stability. ALADIN model is a spectral model for regional forecast of meteorological fields and elements. Its development is being done by a consortium of 16 member countries with Météo-France as a leading partner. ALADIN is used as operational NWP model at the National Institute of Meteorology and Hydrology in Bulgaria more than 20 years and for all these years it has undergone great development.

In the present study, the atmospheric instability over Bulgaria assessed based on the last version of ALADIN-BG forecast production for the warm half-year of 2018 and 2019 is evaluated and connected to the detected lightning. Lightning data are taken from ATDnet (Arrival Time Differencing NETwork), lightning location network of the Met Office (Lee, 1986; Gaffard et al., 2008). The aim of the study is to see if the forecasted instability indices are suitable for lightning probability forecast and if positive, to determine threshold values for the considered forecasted instability indices over Bulgaria for the use of thunderstorm formation probability prediction using the regional NWP model ALADIN-BG. In the next sections of the paper a more detailed description of the instability indices evaluated in the present study (Section 1.1), the NWP model version (Section 1.2), ATDnet (Section 1.3) and the Methodology of the present study (Section 1.4) are presented. Results and conclusions are in Section 2 and Section 3 respectively.

## **1.1. Instability indices**

Instability indices as Lifted Index, Cross Totals index, Vertical Totals index, Total Totals index and K index derived from the thermodynamic parameters, as well as the Severe

Weather Threat Index that includes wind shear parameters were considered for the aim of the present study.

### ***1.1.1. Lifted index***

Developed by Galway (1956), the Lifted index (LI) assesses the degree of stability of the atmosphere between the surface and 500 hPa. It is the difference between the observed temperature at 500 hPa and the temperature of an air parcel that is lifted from the surface to its lifting condensation level (LCL) dry adiabatically and further moist adiabatically to 500 hPa. LI is a forecast index, as a negative LI represents an unstable boundary layer compared to the middle troposphere. A value of 2°C has been used as an upper limit for severe convection, but this varies from location to location. Usually, the following thresholds are considered:

- LI  $\geq$  6 °C - Very Stable Conditions
- 6 °C > LI > 1 °C - Stable Conditions, Thunderstorms Not Likely
- 0 °C > LI > -2 °C - Slightly Unstable, Thunderstorms Possible, With Lifting mechanism (i.e., cold front, daytime heating, ...)
- 2 °C > LI > -6 °C - Unstable, Thunderstorms Likely, Some Severe With Lifting mechanism
- 6 °C > LI - Very Unstable, Severe Thunderstorms Likely With Lifting mechanism

### ***1.1.2. Vertical Totals, Cross Totals and Total Totals***

They are used as a first guess indices to identify the potential for severe convection (Miller, 1972). The Vertical Total index (VT) gives an indication of the vertical temperature gradient of a layer of the atmosphere which includes the top of the boundary layer up to 500 hPa level. It is calculated as the temperature difference between the 850 hPa (T850) and the 500 hPa (T500) levels.

$$VT = T850 - T500$$

Humidity is an important element in the process of deep moist convection in addition to strong vertical temperature gradient. In order to consider the humidity in the calculation, Miller (1972) devised the Cross Total index (CT) which uses the dewpoint temperature at the 850 hPa (Td850) instead of the temperature and is given by

$$CT = Td850 - T500$$

However, in the presence of a steep temperature lapse rate the CT and VT can have large values even if the low level moisture is not high. Such indices must be used with care as they are bound to overestimate the potential of convection. To account for both the depth of moisture in the low level and vertical temperature gradient in the layer, the Total Total index (TT) was proposed as a sum of the CT and VT and is given by

$$TT = VT + CT = T850 + Td850 - 2 T500$$

The TT has shown a high degree of success (Huntrieser et al., 1996) and the thunderstorm threshold varies between 45 and 50 depending on the geographical location, the season and the synoptic situation (Marinaki et al., 2006). The higher the value of TT the higher the probability of thunderstorm is.

### **1.1.3. K index**

The K index was developed by J.J.George (1960). K is a measure of thunderstorm potential based on the vertical lapse rate, moisture content of the lower atmosphere, and the vertical extent of the moist layer. It is derived by:

$$K = (T850 - T500) + Td850 - (T700 - Td700)$$

where T850, T700 and T500 are air temperature at 850 hPa, 700 hPa and 500 hPa and Td850 and Td700 – dewpoint temperature at 850 hPa and 700 hPa. The K index is related to the probability of occurrence of a thunderstorm with usual interpretation:

$K < 20 \text{ }^\circ\text{C}$	– none thunderstorm probability
$20 \text{ }^\circ\text{C} \leq K \leq 25 \text{ }^\circ\text{C}$	– isolated thunderstorms
$25 < K \leq 31 \text{ }^\circ\text{C}$	– widely scattered thunderstorms
$31 < K \leq 35$	– scattered thunderstorms
$35 < K$	– numerous thunderstorms

## **1.2. ALADIN-BG model**

The ALADIN (Aire Limitée Adaptation Dynamique Développement International, International development for limited-area dynamical adaptation) System is the set of pre-processing, data assimilation, forecast model and post-processing – verification software codes shared and developed by the partners of the ALADIN consortium to be used for running a high-resolution limited-area model (LAM) for producing the best possible operational numerical weather prediction (NWP) applications based on a configuration compatible with their available computing resource (Termonia et al., 2018). Bulgaria through the National Institute of Meteorology and Hydrology (NIMH) is in the ALADIN consortium since 1992, and the LAM model ALADIN is operational in the institute since 1999. ALADIN uses a spectral dynamical core with a two-time level semi-implicit semi-Lagrangian scheme. Nowadays, the operational model configuration at NIMH is the following: the integration domain is covering a big part of the Balkan Peninsula, centered on Bulgaria, with a horizontal resolution of 5 km, 105 vertical levels, a time step of 300 s and a forecast range of 72 h. It is run twice daily, at 06 and 18 UTC and it uses the global ARPEGE of Météo-France (Courtier and Geleyn, 1988; Courtier et al., 1991) output for initial and boundary conditions. Since November 2019, the operational model is based on cy43t2. However, the actual study, as based on data

from the summer of 2018 and 2019, uses forecast data obtained with cy41t1, version older than the current operational model in the institute.

### 1.3. ATDnet

In the present study lightning data are based on data from ATDnet (Arrival Time Differencing NETwork) over the territory of Bulgaria for the period 2018-2019. ATDnet is the most recent version of the VLF (very low frequency) lightning location network of the Met Office that operates since 1987 (Lee, 1986; Gaffard et al., 2008). It takes advantage of the long propagation paths of the VLF spherics emitted by lightning discharges, which propagate over the horizon via interactions with the ionosphere. The differences in the arrival times of these strokes at the outstations are used to calculate the lightning's location. ATDnet predominantly detects spherics created by cloud to ground (CG) strokes, as the energy and polarization of spherics created by CG return strokes mean that they can travel more efficiently in the Earth-ionosphere waveguide, and so are more likely to be detected at longer ranges than typical inter-/intracloud (IC) discharges (Anderson and Klugmann, 2014). Data are collected every minute and BUFR encoded using the 'Universal BUFR template for lightning data' with 15 minutes of data combined into one file which is then sent by the UK Met Office on behalf of the World meteorological organization to member states through its Global telecommunication system. The study on lightning density over Europe using 5 years of ATDnet data (between 2008 and 2012) performed by Anderson and Klugmann showed that the highest concentration of the detected lightning flashes over the region of Bulgaria is during June (when Bulgaria, Romania and northern Italy demonstrate the highest lightning densities in Europe) and July. Our preliminary results (not published yet) on data from ATDnet for the period 2012-2020 confirmed that 40% of all detected flashes over Bulgaria are during June and July (28 % for June and 22% for July).

For the aim of the present study, ATDnet lightning data over the domain that covers 41N - 44.4N and 22E - 28.9E are evaluated within the model grid with a resolution of 0.05x0.05deg for the warm half-year period of 2018 and 2019. ATDnet fixes that occurred within 5 km of and within 1 s after another fix were grouped together as a single flash. These criteria should capture the majority of fixes that occur within spatially extensive flashes, or strokes within the same flash where the error on one or more of the strokes were mislocated by a few kilometres (Anderson and Klugmann, 2014). The location and time of the first fix in the group of fixes were used as the location and time of the flash. Forecast and lightning data are considered on the base of a 3 hours time period over the domain shown in Figure 1, which means that one day consists of 73728 bins (9591 domain grids points x 8 three hours time intervals), a warm half-year - of 14041224 bins (73728 bins x 183 days). For the whole considered period from April to September of 2018 and 2019, 28082448 bins were processed independently (as a first step) for the purpose to determine threshold values for the forecast stability indices over

Bulgaria to be used for thunderstorm formation probability prediction with the regional NWP model ALADIN-BG.

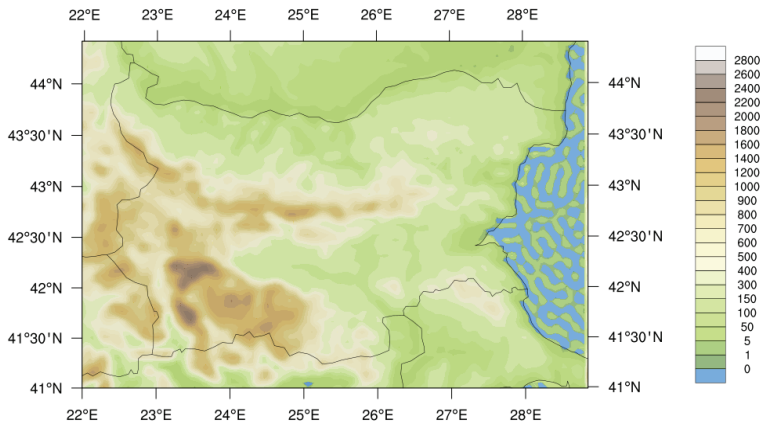


**Fig. 1.** Post-processed model altitude of the area over which the relationship between forecast instability indices and lightning data has been studied.

## 1.4. Methodology

As a beginning, indices LI, K, CT, VT, and TT for the warm half year (from April to September) of 2018 and 2019 derived from ALADIN-BG were validated with the corresponding ones derived from the vertical sounding over Sofia. Model (taken from the closest in time forecast) and sounding data for instability indices were considered for three samples of data – data for cases without any detected flashes (denoted as “no light”, data for cases with 1 to 4 detected flashes (denoted as “light” cases), and data for cases with more than 4 detected flashes (denoted as “more light”). The arbitrary separation of cases “light” from “more light” was in an attempt to estimate also the relationship between the instability indices and the severity of the thunderstorms.

The second part of the study consists of a monthly and diurnal evaluation of the model instability indices for the three samples of data “no light”, “light” and “more light” with taking into account additionally the forecast range. The last is important to establish whether different forecast overlap, and to which extend of the forecast range instability indices are reliable for thunderstorm forecast. All results in these parts of the study are shown on boxplots giving information for extreme values of data samples, their median, and their first and third quartiles. The number of all considered corresponding bins used for the statistical analysis is indicated in Table 1 in the Appendix.

As statistical analysis did not show an important separation of cases “light” and “more light”, all cases with lightning were merged for the next part of the study. Based on 25<sup>th</sup> and 75<sup>th</sup> percentiles of samples for data without and data with detected flashes, threshold

values for the instability indices LI, K and TT were proposed for the forecast of high, medium and low lightning probability. Further, the monthly Hit Rate or Probability of detection (POD) and False alarm ratio (FAR) for thunderstorm forecast during 2018-2019 warm-half year based on LI, KI and TT threshold values are then considered for the different forecast. POD for instability indices during May 2020, calculated with the new operational version of ALADIN-BG is determined with the aim to test how passing from one version to another affects the results and if the previously determined threshold values were adequate for the new version.

## 2. RESULTS

In order to validate model data for the studied instability indices with the real ones, the corresponding model data with those derived from vertical sounding over Sofia were compared. This only radiosonde measurements in Bulgaria are performed once daily, at 12 UTC, and since June 2019 additionally at 06 UTC at NIMH. Figures 2 – 4 show the warm half year of 2018 and 2019 distribution of Lifted Index (LI), Vertical (VT), Cross (CT) and Totals (TT) Total Indices, and K (KI) indices for Sofia station based on radiosonde data and model data, and for the whole domain based on model data. As ALADIN forecast range is 72 hours, for each time interval there are 6 corresponding forecasts, from the six previous model runs. As a beginning, we consider the closest in time forecast data or as we will call it later, the first forecast. All cases are separated into three groups: without (“no light”), with one to five (“light”) and with more than five (“more light”) detected flashes in an attempt to estimate additionally the relationship between the instability indices and the severity of the thunderstorm. The number of cases “no light” for Sofia station is 340, for “light” - 20 and for “more light” - 7. As expected, the disproportionate nature of the data samples is similar for the whole domain – 22738422 for “no light”, 342979 for “light” and 59670 for “more light”. About 5000000 from the initial bins were excluded from the statistics due to data inconsistencies (mainly due to lack of a corresponding forecast). Regardless of the disparities of the samples, all other consistent data were considered as the aim of the study is mainly to test the use of model data (with their relative uncertainties) for the correct thunderstorm forecast. Results show that data for LI, VT, CT, TT and KI from ALADIN-BG correlate very well to those from the radiosonde measurements (with correlation coefficients R respectively 0.91, 0.94, 0.89, 0.93 and 0.88). The median of LI derived from radiosonde data and from model over Sofia for “no light” cases is 1.7°C and 0.1°C respectively, while for the whole domain (LI from model data) – 0.93°C (Figure 2, left). For “light” cases the respective sample medians are -1.1°C, -4°C and -4.3°C, and for “more light” cases -1.78°C, -5.3°C and -5°C. This shows a slight relationship between thunderstorm severity and LI. Also, results show that regardless the good correlation between the two sets of data over Sofia, model data are slightly lower than the measured ones. The 1<sup>st</sup> quartile of radiosonde data for “no light” is -0.1°C, while

the corresponding 3<sup>rd</sup> quartiles for “light” and “more light” are respectively  $-0.3^{\circ}\text{C}$  and  $-1.1^{\circ}\text{C}$ , which shows a good discrimination of 75 % of LI for cases with and without detected lightning. For LI over Sofia derived from model data the 1<sup>st</sup> quartile for “no light” is  $-2.7^{\circ}\text{C}$ , while the corresponding 3<sup>rd</sup> quartiles for “light” and “more light” are respectively  $-2.4^{\circ}\text{C}$  and  $-2.6^{\circ}\text{C}$ . In this case, less than 75 % of values of LI for cases with and without lightning are well separated. However, for the whole domain, model data for LI discriminate correctly in cases with or without lightning also more than 75% of all cases (as the 1<sup>st</sup> quartile for “no light” is  $-2.2^{\circ}\text{C}$ , while the 3<sup>rd</sup> quartile for “light” and “more light”  $-2.4^{\circ}\text{C}$  and  $-2.6^{\circ}\text{C}$ ). Results for VT (Figure 2, right) show that a better discrimination of cases with and without lightning is obtained with model data in comparison to the measured ones, at least for Sofia data. Although data samples medians for VT from radiosonde measurements show a slight increase for lightning cases ( $26.3^{\circ}\text{C}$ ,  $27.5^{\circ}\text{C}$  and  $28.5^{\circ}\text{C}$  respectively for cases “no light”, “light” and “more light”), the 3<sup>rd</sup> quartile for “no light” cases is  $28.35^{\circ}\text{C}$ , while the 1<sup>st</sup> quartiles for “light” and “more light” are  $25.75^{\circ}\text{C}$  and  $25.4^{\circ}\text{C}$ . There is an undetermined interval of about  $3^{\circ}\text{C}$  (cases of VT between  $25^{\circ}\text{C}$  and  $28^{\circ}\text{C}$ ) that could correspond to a thunderstorm situation, as well as to a non-thunderstorm situation. Similar is for VT based on model data, with a slight increase of median for lightning data of VT ( $26.3^{\circ}\text{C}$ ,  $27.4^{\circ}\text{C}$  and  $28.2^{\circ}\text{C}$  respectively for “no light”, “light” and “more light” cases over Sofia domain, and  $26.2^{\circ}\text{C}$ ,  $27.1^{\circ}\text{C}$  and  $27.2^{\circ}\text{C}$  for the whole domain). Analogical is the distribution of CT (Figure 3, left). However, there is no differentiation between CT data derived from model for cases “light” and “more light”, even cases with more than 5 detected lightning tend to correspond to lower values of CT in comparison to cases with 1 to 5 lightning.

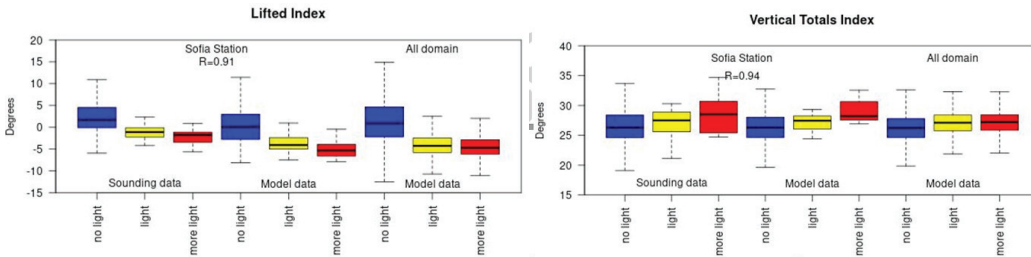


**Fig. 2.** Boxplots of Lifted Index (left panel) and of Vertical Totals Index (right panel) for 2018-2019 (warm half-year) : the first 6 boxes correspond to data for Sofia station – derived from radiosonde measurements and from model forecast fields (with indicated correlation coefficient  $R$  between the two sets of data), the last three boxes correspond to data derived from model forecast fields for the whole considered domain (no light – cases without any detected flashes (blue), light – cases with 1 to 4 detected flashes (yellow), more light – cases with more than 5 detected flashes (red))

The distribution of TT (Figure 3, right) over the whole domain shows that medians for respectively “no light”, “light” and “more light” cases are  $46.1^{\circ}\text{C}$ ,  $49.7^{\circ}\text{C}$  and  $49.8^{\circ}\text{C}$ , with an undetermined interval of about  $2^{\circ}\text{C}$ , as the 3<sup>rd</sup> quarter for “no light” cases is

49.2°C, while the 1<sup>st</sup> quarters for “light” and “more light” cases are equal to 47.4°C. In contrast to CT, VT and TT, for which median values for the different corresponding groups over Sofia are close when derived from radiosonde measurements or from the model, model median values for KI (Figure 4) are lower than radiosonde ones (26.9°C versus 27.7°C for “no light”, 31.7°C versus 34.4°C for “light” and 31.5°C versus 34.2°C for “more light”) as was the case for LI.

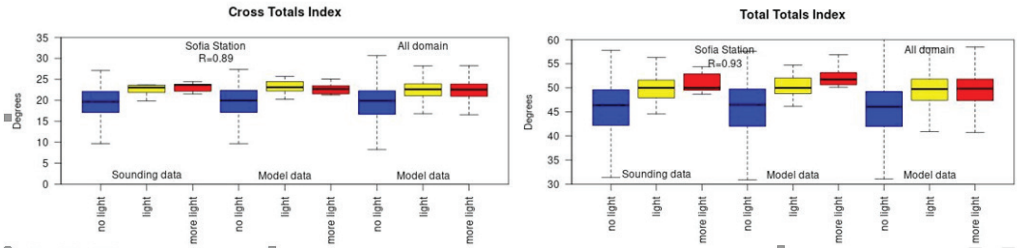


**Fig. 3.** Boxplots of Cross Totals Index (left panel) and of Total Totals Index (right panel) for 2018-2019 (warm half-year): rest as in Figure 2

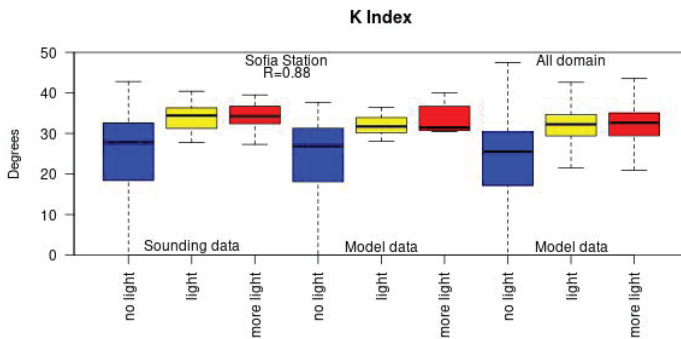


**Fig. 4.** Boxplot of K Index for 2018-2019 (warm half-year): rest as in Figure 2

Having in mind that the considered instability indices are based on thermodynamic conditions in the atmosphere that depend on diurnal and seasonal atmospheric state, instability indices for cases “no light”, “light” and “more light” were considered for the different diurnal hours intervals and months. Also, as mentioned above, ALADIN forecast range is 72 hours ahead and for each time interval there are 6 corresponding forecasts, from the six previous model runs. It is important to establish whether different forecasts overlap, and also to which extend of the forecast range instability indices are reliable for thunderstorm forecast. Figures 5 - 10 show boxplots of Lifted Index LI for cases without any detected flashes, cases with 1 to 4 detected flashes, and cases with more than 4 detected flashes as a function of the forecast range for the different model runs (at 06 UTC and at 18 UTC) for different months. A pronounced diurnal

trend is visible for all months for the two corresponding model runs. Values of LI for the three considered groups are visibly lower for daily hours in comparison to LI values during night hours independently of the forecast range. In April (Figure 5) a very good discrimination of thunderstorm cases from the non-thunderstorm ones for the daily hours, while no significant differentiation for night cases are visible. Even for the closest to the forecast night hours (between 18 h and 24 h after the 06 UTC run and between 6 and 9 hours after the 18 UTC run) LI values for thunderstorm cases are higher than those for non-thunderstorm cases. That could be due to the significantly small number of thunderstorm cases bins in comparison to the non-thunderstorm cases bins in April during 2018 and 2019 that could lead to a more tangible weight of certain inaccurate forecast for thunderstorm. In May (Figure 6) the number of thunderstorm cases increases and there is still a visible differentiation in the distributions of LI for the cases in the three groups as for daily hours, as well for night hours, even with higher night values of LI obtained with the two model runs (at 06 and 18 UTC). During the months June (Figure 7) and July (Figure 8), with the established heat, major driving factor in case of large scale atmospheric dynamics in favoring the overall atmosphere instability, the differentiation of cases with lightning from those without tends to blur, especially in July. A decrease of LI values for all cases in comparison to other months is noticeable. In August (Figure 9) and September (Figure 10) as the whole atmosphere tends to be more stable over Bulgaria in comparison to June and July, the distinction between thunderstorm and non-thunderstorm cases becomes more visible.

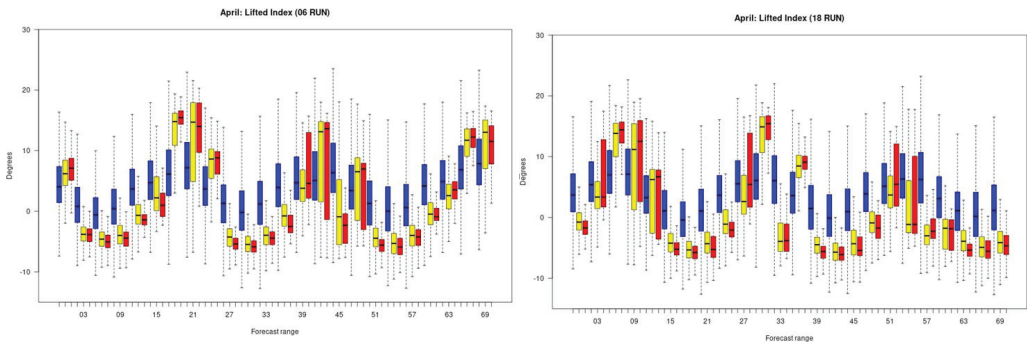


**Fig. 5.** Boxplot of Lifted Index for cases without any detected flashes (blue), cases with 1 to 4 detected flashes (yellow), and cases with more than 4 detected flashes (red) as a function of the forecast range for the model runs at 06 UTC (left) and 18 UTC (right) for April 2018-2019

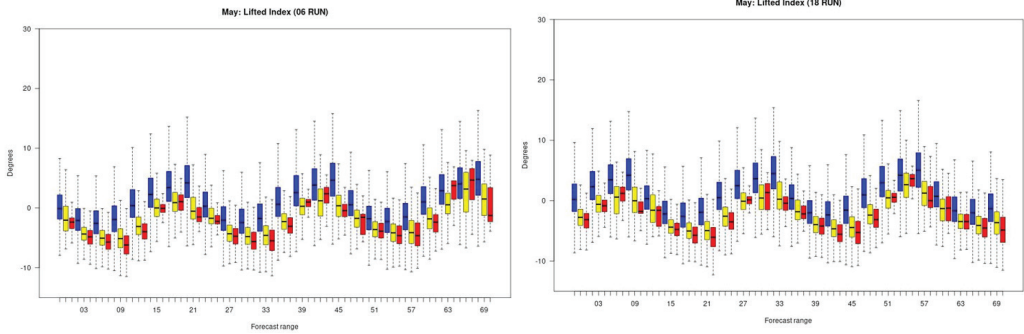


Fig. 6. Same as Figure 5 but for May 2018-2019

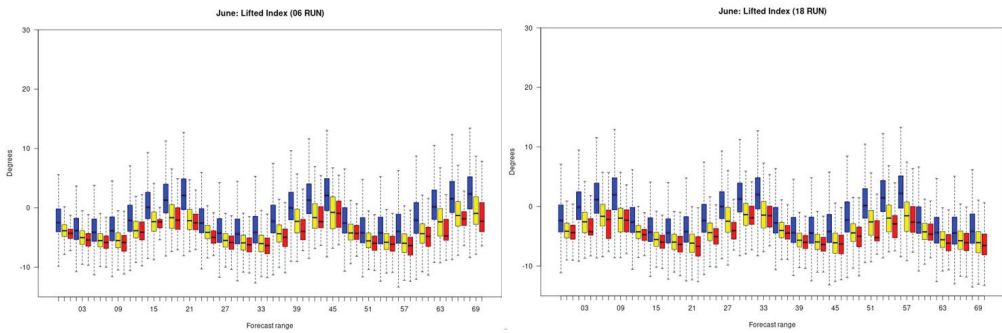


Fig. 7. Same as Figure 5 but for June 2018-2019

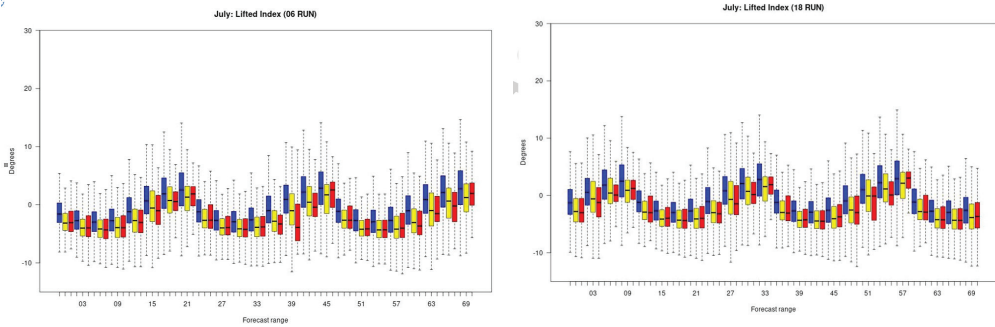
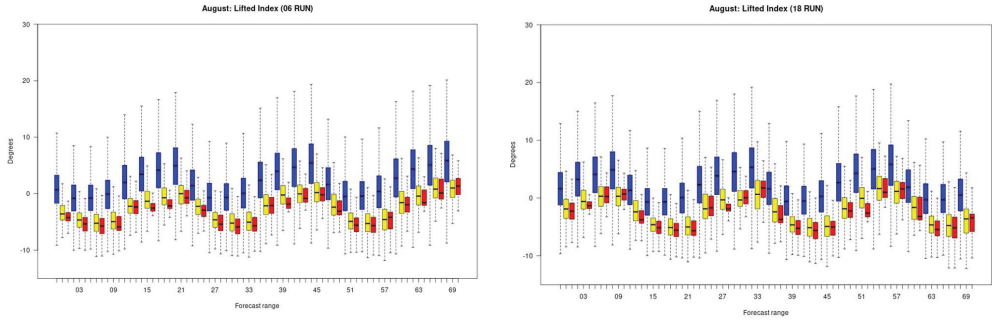
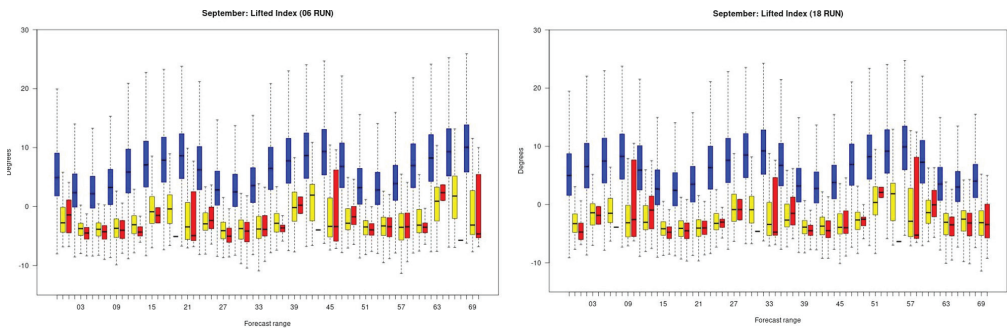


Fig. 8. Same as Figure 5 but for July 2018-2019



**Fig. 9** Same as Figure 5 but for August 2018-2019



**Fig. 10.** Same as Figure 5 but for September 2018-2019

The results are similar for the other considered instability indices, except that there is not a so pronounced difference in their diurnal distribution. Figure 11, left shows the monthly distribution of TT for daily hours (between 06 and 18 UTC) for the cases without any detected flashes, cases with 1 to 4 detected flashes, and cases with more than 4 detected flashes. There is a good discrimination between values of TT for thunderstorm and non-thunderstorm cases during April, May, August and September, and a weaker one in June and July, when thunderstorm values of TT seem to be smaller with  $\sim 2^{\circ}\text{C}$  in comparison to other months. However, there is no significant differentiation between cases with up to 4 and with more than 4 detected flashes, which is more significant in case of LI. Similar to TT is the distribution of CT, VT (not shown here) and KI (Figure 11, right), except that the mean thunderstorm values of KI are identical for April, May, June and July, while in August and September they are with  $\sim 2^{\circ}\text{C}$  higher.

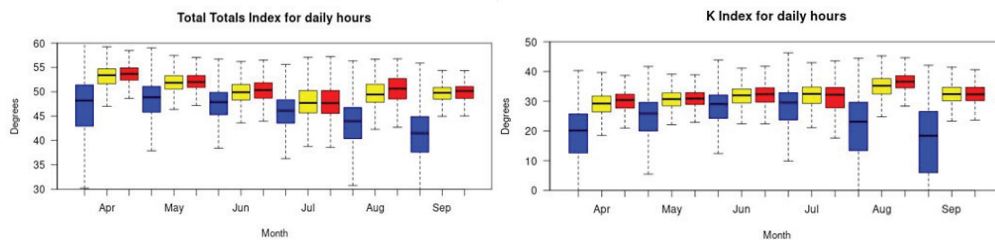


**Fig. 11.** Boxplot of Total Totals Index (left panel) and of K Index (right panel) for the daily hours (between 06 and 18 UTC) for cases without any detected flashes (blue), cases with 1 to 4 detected flashes (yellow), and cases with more than 4 detected flashes (red) during the warm - half year of 2018 and 2019

As statistical analysis did not show an important separation of cases “light” and “more light”, all cases with lightning were merged for the next part of the study. Based on simple statistical analyses, and more precisely considering “no light” and “light” data samples extreme quartiles values, threshold values for LI, TT and KI (Table 1, Table 2 and Table 3 respectively) are obtained for the following conditions:

- $TT/KI (LI) > (<) B$  – high thunderstorm probability
- $A < (>) TT/KI (LI) < (>) B$  – moderate thunderstorm probability
- $A > (<) TT/KI (LI)$  – low thunderstorm probability

The threshold values for the different months and for LI, additionally for the day and night are proposed.

**Table 1.** Threshold values for the Lifted Index (A is derived as the 25<sup>th</sup> quartile value for “no light” sample, while B – the 75<sup>th</sup> quartile of the “light” cases sample)

	Day		Night	
	A	B	A	B
April	-1	-2	3	2
May	-3	-4	0	-1
June	-4	-5	-1	-3
July	-2	-4	1	-2
August	-2	-4	1	0
September	-2	-3	2	0

Figures 12 – 14 show the monthly Hit Rate or Probability of detection (POD) and False alarm ratio (FAR) for thunderstorm forecast during 2018-2019 warm-half year based on LI, KI and TT threshold values respectively in Tables 1 – 3 for the different forecast. Here cases with “high” and “medium” lightning probability are considered as cases with forecasted lightning probability, while cases with “low” lightning probability – as no forecasted lightning probability. Then POD is the fraction of observed events that

were forecasted correctly and FAR is the fraction of “yes” forecasts that were wrong, i.e., were false alarms. They are calculated as follows:

**Table 2.** Threshold values for the Total Totals Index

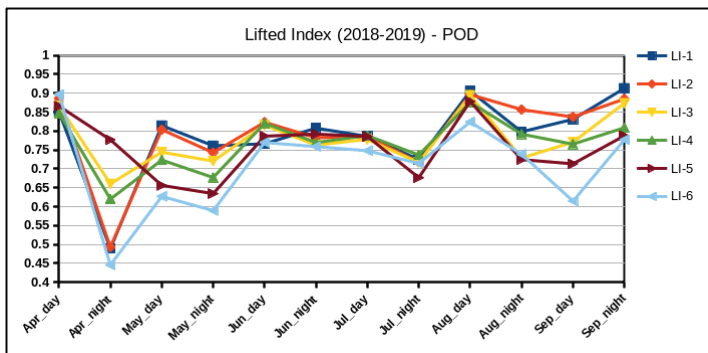
	A	B
April	50	52
May	50	52
June	48	50
July	45	50
August	46	50
September	44	48

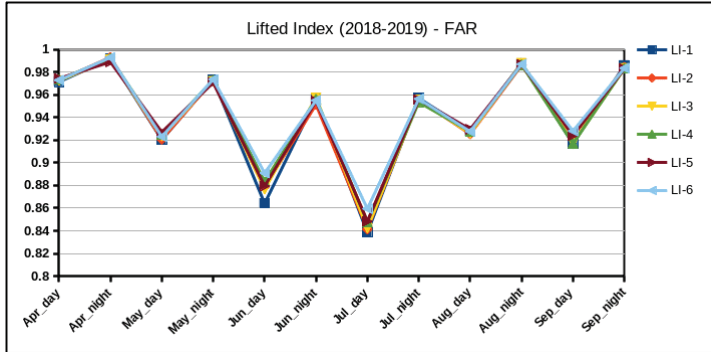
**Table 3.** Threshold values for the K Index

	A	B
April	26	27
May	28	30
June	29	33
July	27	33
August	29	32
September	27	30

$POD = a/(a+c)$ , where  $a$  – is the number of forecast thunderstorm that occurred (or number of cases with detected lightning and forecast index higher (or lower in case of LI) than A;  $c$  – is the number of not forecast thunderstorm that occurred (or number of cases with detected lightning and forecast index lower (or higher in case of LI) than A.

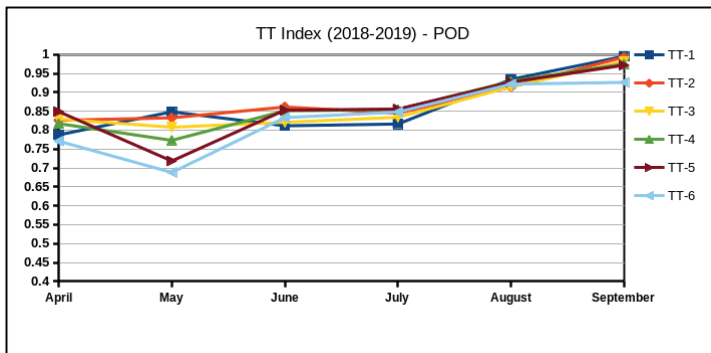
$FAR = b/(a+b)$ , where  $b$  – is the number of forecast thunderstorm that did not occur (or number of cases with no detected lightning and forecast index higher (or lower in case of LI) than A.

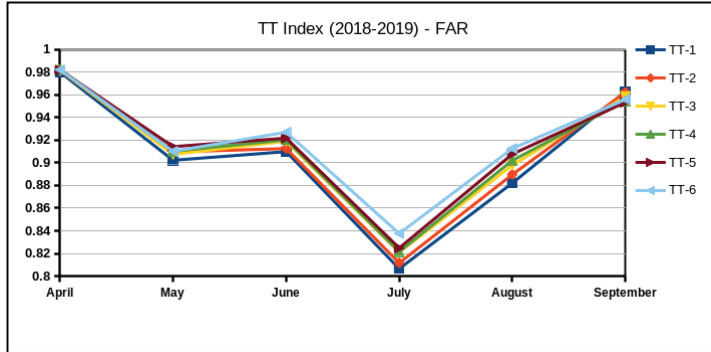




**Fig. 12.** Monthly Hit Rate or Probability of detection POD (top panel) and False alarm ratio – FAR (bottom panel) for thunderstorm forecast during 2018-2019 warm-half year based on Lifted Index threshold values in Table 1 for the different forecast (LI -1 is the closest, while LI-6 the farthest in time)

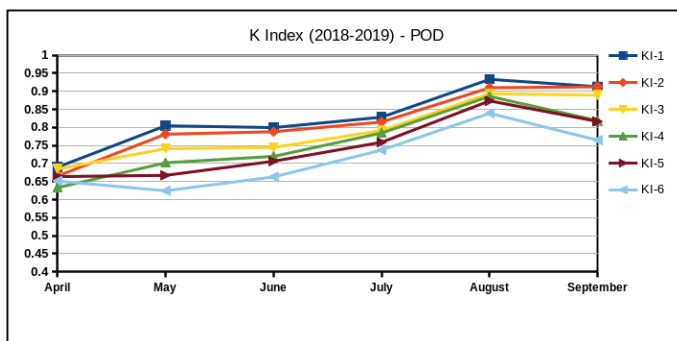
It has to be stressed that the non thunderstorm bins are more than 98% of all considered bins, while only less than 2% are thunderstorm bins. This significant prevail of the number of cases without lightning strongly affects the results for FAR that are above 0.8 for all considered indices. For threshold values of LI (Figure 12) the mean value of POD is 0.77, with higher values for day forecast. The best probability of detection is observed in August when POD is about 0.9 for all forecast, except of the farthest LI-6 (with POD=0.83). In June and July (day and night) and April and August (day), all 6 forecasts for LI give similar values of POD, while in April and August (night) and May and September (day and night) the probability of detection based on LI is different depending of the remoteness in time of the forecast. Usually the first two forecasts are with higher POD, but in April (night) POD=0.78 for LI-5, while for LI-1 and LI-2 POD=0.5. The effect of the remoteness of time of the forecast is not visible in case of the false alarm detection for LI threshold values. FAR is lower for day forecast in comparison to night forecast, and the best results for FAR are obtained in June and July (the months with higher number of thunderstorm bins).





**Fig. 13.** The same as Figure 12 but based on Total Totals Index threshold values in Table 2 for the different forecast (TT -1 is the closest, while TT-6 the farthest in time)

For threshold values of TT (Figure13) the mean value of POD is 0.86, with highest values in September (0.98). The difference of POD between all forecasts for June, July and August does not exceed 0.1, while in May there is a visible effect of the different forecast on POD, showing better results by zooming in time. In June and July, the closest forecasts have lower POD. In July, FAR for TT thresholds values is the lowest, also showing better results by zooming in time. In general, FAR for TT is more dependent on the forecast remoteness in comparison to FAR for LI. Identical is the behavior of POD for KI threshold values (Figure 14), as with time, thunderstorm forecast deteriorates, and this for all considered months. The best results in forecasting lightning probability with KI are obtained in August, and the worst in April. The mean value of POD for thresholds values of KI is 0.77. June and July are with best results for FAR for KI, as a dependence on the remoteness in time of the forecast is visible only in June.



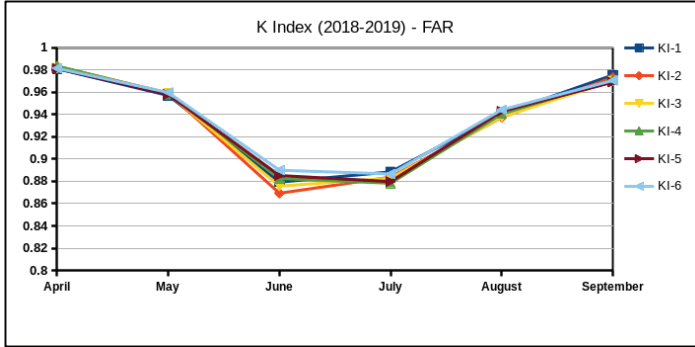


**Fig. 14.** The same as Figure 12 but based on K Index threshold values in Table 3 for the different forecast (KI -1 is the closest, while KI-6 the farthest in time)

As mentioned above, all the study presented here is based on data from the warm half year for 2018 and 2019. During this time the operational version of ALADIN-BG was based on cy41t1. Since November 2019, we switched on cy43t2. It is worth to test how passing from one version to another affects the results and are the previously determined threshold values adequate for the new version. For this aim, we tested POD and FAR using thresholds values (obtained based on data from 2018-2019) of LI, KI and TT for May 2020. Figure 15 compares POD for thunderstorm forecast based on LI, TT and KI threshold values during May 2018-2019 and during May 2020 as a function of the different forecasts. It is visible that only for KI there is a deterioration of POD when using the new cy43t2 and the remoteness in time of the forecast is kept. For LI and TT, POD obtained for May 2020 is higher and the effect of the remoteness of the forecast is less pronounced in comparison to May 2018-2019. Results for FAR (not shown here) for May 2020 are similar to those for May 2018-2019 for all considered indices.

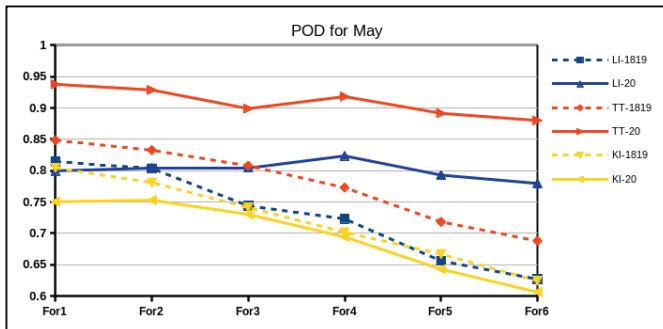


**Fig. 15.** Probability of detection POD for thunderstorm forecast based on LI, TT and KI threshold values during May 2018-2019 (-1819, obtained with cy41t1) and during May 2020 (-20, obtained with cy43t2) as a function of the different forecasts (For1 is the closest, while For6 the farthest in time)

### **3. DISCUSSION AND CONCLUSION**

For the present study, ATDnet lightning data over the domain are evaluated within the model grid with a resolution of  $0.05 \times 0.05$  deg. That means that fixed data were interpolated into the model grid. Furthermore, it has to be stressed that to consider a case as a “thunderstorm case” at least one flash has to be detected in the vicinity of the considered grid point (as cases were considered to perform the statistical analyses), which is a very strong restriction, even without mentioning the location accuracy of ATDnet lightning detection or its detection efficiency. The study is directed to indices that are able to determine the instability of the atmosphere and the possibility for thunderstorm to develop and therefore to have a lightning activity, that is not always the case. Figure 16 shows an example of a day (02/05/2020) with several local thunderstorms developed over different regions in Bulgaria and surroundings and the corresponding forecast from 02/05/2020 at 06 UTC for LI. As visible from the figure, for 02/05/2020 at 06 UTC over the western part of Bulgaria LI values are higher than  $-2^{\circ}\text{C}$ , while over the central and eastern parts – lower. At the same picture, some black points, representing the flashes detected between 06 and 09 UTC are distinguished at the border line between Bulgaria and Turkey, and over the central south part.

Satellite images for the same time period (Figure 17) show that clouds formed over the central and especially eastern part of the country. More flashes are detected between 09 and 12 UTC (picture for 02.05.20 - 09 UTC) where LI was forecasted to be around  $-5^{\circ}\text{C}$  or lower. However, from this figure it is visible that only a little part of cases with  $\text{LI} < -5^{\circ}\text{C}$  are considered as “thunderstorm cases”, while from Figure 17 for 02/05/2020 1200 UTC we see that cloud cover over Bulgaria is similar to the forecasted. Flash density for 02.05.20 – 15 UTC is lower in comparison to 12 UTC, while more cases are with LI around  $6^{\circ}\text{C}$ . At 02/05/2020 1800 UTC (Figure 17) some convective cases are well visible over the whole considered region. There are also several flashes detected between 18 and 21 UTC on 02/05/20, but they are mostly concentrated on two main mesoscale convective systems (one formed over Bulgaria and other – over Turkey). Thus, almost all other cases are considered as “non thunderstorm” cases in the statistical analyses in the present study. During the night (between 21 and 06 UTC) several flashes were detected over the eastern border and over the Black Sea, where LI forecasted values are around  $0^{\circ}\text{C}$ . Other parts over the considered region are with lower values of LI, with no detected flashes, however with clouds visible on corresponding satellite images.

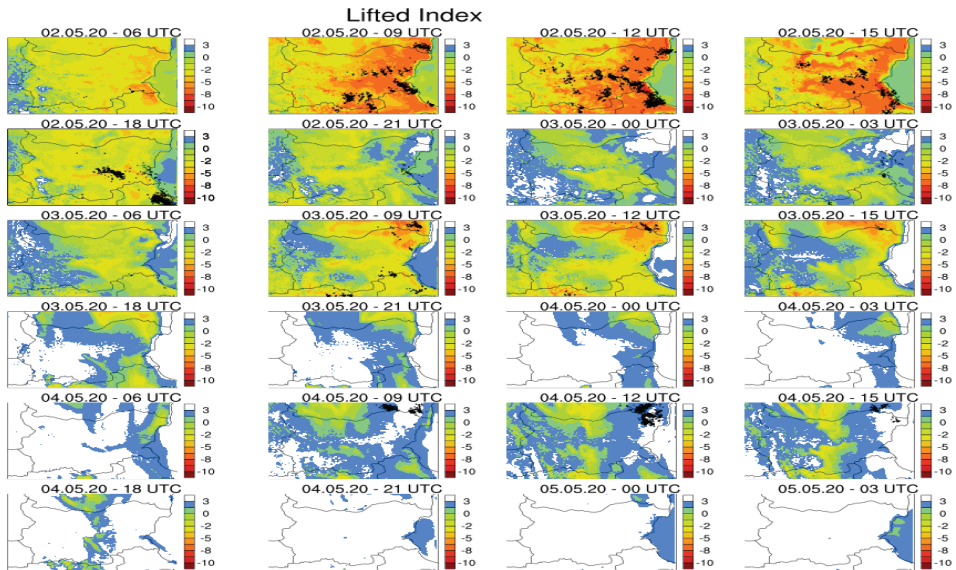


**Fig. 16.** Lifted Index forecast on 02.05.2020 (06 UTC Run) with the corresponding lightning data detected by ATDnet

This case is a good illustration that: 1) the instability indices are not the best predictor for lightning activity, and more precisely for the accurate determination of its location; 2) a big part of FAR cases are considered as false alarms (in the frame of the present study), while in fact they more often correspond to convective cases with no detected flashes (that could be detected in their vicinity). It has to be stressed that in the reality, thunderstorms are related to the instability in the atmosphere, but not always the atmospheric instability leads to thunderstorm formation. That is why we believe that looking for spatio-temporal neighborhood of lightning observations (Theis et al., 2005, Berocal et al., 2007, Schwartz and Sobash, 2017, and others) for the validation of the forecasted instability indices will not improve significantly the results. Furthermore, it is accepted that the large-scale indices tend to “hedge” forecasts by overpredicting the area at risk of lightning (Wilkinson, 2017). However, all considered here indices showed a relatively good ability to discriminate thunderstorm cases from the non thunderstorm ones, depending on the month. Results presented in the different boxplots for the different instability indices, as well the results for the probability of detection based on their thresholds values confirmed that LI, TT (and its derivatives VT and CT) and KI obtained based on NWP model data could be considered for predicting the atmospheric instability and therefore, for the possibility to thunderstorm formation over different regions. Although, they should not be used as a sole tool for a more accurate in space and time thunderstorm forecast.

*On the use of atmospheric instability indices based on NWP model production for thunderstorm forecast*

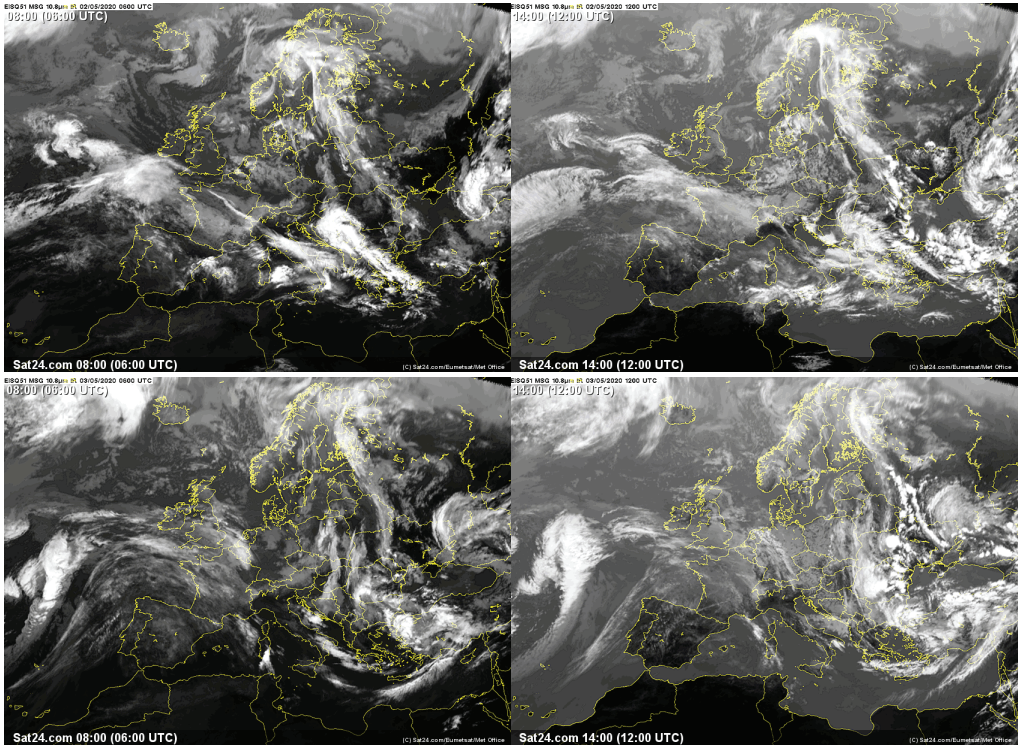


**Fig. 17.** Satellite images (IR) for 02.05.2020 (at 06 and 12) and 03.05.2020 (at 06 and 12 UTC) (taken from [www.sat24.com](http://www.sat24.com))

## REFERENCES

- Anderson, G. and Klugmann, D., (2014), European lightning density using ATDnet data, *Nat. Hazards Earth Syst. Sci.*, 14, 815–829, 2014.
- Berrocal, V. J., Raftery, A. E. and Gneiting, T., (2007), Combining spatial statistical and ensemble information in probabilistic weather forecasts. *Mon. Weather Rev.* 135, 1386–1402.
- Courtier, P. and Geleyn, J.-F., (1988), A global numerical weather prediction model with variable resolution: Application to the shallow model equations, *Q. J. Roy. Meteor. Soc.*, 114, 1321–1346.
- Courtier, P., Freydier, C., Geleyn, J.-F., Rabier, F., and Rochas, M. (1991), The ARPEGE project at Météo-France, *Proceedings of 1991 ECMWF Seminar on Numerical Methods in Atmospheric Mod-els*, ECMWF, Reading, UK, 193–231.
- Doswell, C. A. III, and D. M. Schultz, 2006: On the use of indices and parameters in forecasting severe storms. *Electronic J. Severe Storms Meteor.*, 1(3), 1–22.

- Gaffard, C., Nash, J., Atkinson, N., Bennett, A., Callaghan, G., Hibbett, E., Taylor, P., Turp, M., and Schulz, W., (2008), Observing lightning around the globe from the surface, in: the Preprints, 20th International Lightning Detection Conference, Tucson, Arizona, 21–23.
- Galway, J.G., 1956, The lifted index as a predictor of latent instability, *Bull. Amer. Meteor. Soc.*, 37, 528-529.
- George, J., (1960), *Weather Forecasting for Aeronautics*, Academic Press, New York.
- Huntrieser, H., H. Schlager, P. van Velthoven, P. Schulte, H. Ziereis, U. Schumann, F. Arnold, and J. Ovarlez, In-situ trace gas observations in dissipating thunderclouds during POLINAT, paper presented at 12th International Conference on Clouds and Precipitation, Int. Assoc. of Meteorol. and Atmos. Sci., Zurich, Switzerland, 1996.
- Lee, A. C., (1986), An operational system for the remote location of lightning flashes using a VLF arrival time difference technique, *J. Atmos. Oc. Technol.*, 3, 630–642.
- A. Marinaki, A., Spiliotopoulos, M., Michalopoulou, H., (2006) Evaluation of atmospheric instability indices in Greece, *Advances in Geosciences*, European Geosciences Union, 7, pp.131-135.
- Markova, B., (2013), *The impact of the environmental conditions on thundercloud formation over Western Bulgaria*, PhD thesis.
- Markova, B., Mitzeva, R., Dimitrova, Ts, (2015), Is there a difference in the environmental conditions at the development of severe and non-severe hailstorms over Bulgaria?, proceeding of 8th European Conference on Severe Storms – ECSS2015, September 14-18, 2015, Wiener Neustadt, Austria.
- Miller, R., (1967), Notes on analysis and severe storm forecasting procedures of the Military Weather Warning Center, Report: Technical Report 200, AWS, USAF: Scott AFB, IL13.
- Schwartz, C. S. and Sobash, R. A. 2017. Generating probabilistic forecasts from convection-allowing ensembles using neighborhood approaches: a review and recommendations. *Mon. Weather Rev.* 145, 3397–3418.
- Termonia, P., Fischer, C., Bazile, E., Bouyssel, F., Brožková, R., Bénard, P., Bochenek, B., Degrauwe, D., Derková, M., El Khatib, R., Hamdi, R., Mašek, J., Pottier, P., Pristov, N., Seity, Y., Smolíková, P., Španiel, O., Tudor, M., Wang, Y., Wittmann, C., Joly, A., (2018), The ALADIN System and its canonical model configurations AROME CY41T1 and ALARO CY40T1, *Geosci. Model Dev.*, 11, 257–281.
- Theis, S. E., Hense, A. and Damrath, U. 2005. Probabilistic precipitation forecasts from a deterministic model: a pragmatic approach. *Meteorol. Appl.* 12, 257–268.
- Tsenova, B and Kolev, ., (2008), Climatological study of the relationships between thunderstorms lightning activity and the environmental conditions over western Bulgaria, Preprints: 15th International Conference of Clouds and Precipitation, Cancun-Mexico.
- Tsenova, B. and Bogatchev, A., (2012), Evaluation of instability indices computed using ALADIN-BG output and their relationship with the thunderstorm activity over Bulgaria, Preprints: 15th International Conference of Clouds and Precipitation, Leipzig, Germany.
- Wilkinson, J.M., 2017, A Technique for Verification of Convection-Permitting NWP Model Deterministic Forecasts of Lightning Activity, *Wea. Forecasting* (2017) 32 (1): 97–115.

**Appendix: Number of bins used for the basic statistical analysis.**

**Table** Number of cases “no\_light”, “light” and “more\_light” for the different hours intervals for the different months

	00-03	03-06	06-09	09-12	12-15	15-18	18-21	21-24	Time	
April	305804	296192	315596	314246	302712	307728	324626	315895	no_	light
	1009	1058	846	2016	3642	1878	1394	564	light	
	99	71	60	241	558	171	74	44	mor	e_
May	516728	516216	525957	516788	508769	514343	520504	525535	no_	light
	1094	1508	1443	9462	16883	11885	6240	1808	light	
	92	190	105	1255	1853	1277	761	162	mor	e_
June	476645	477066	494347	466200	438285	453817	477195	465993	no_	light
	2530	1943	3525	26981	35636	21181	9990	3755	light	
	375	541	860	5551	6207	4552	1956	211	mor	e_
July	532892	532572	530056	499238	484281	503702	521560	531899	no_	light
	3826	3757	5726	31080	44650	27638	13427	5064	light	
	378	767	1314	6778	8165	5756	2109	133	mor	e_
August	507663	507432	516857	512399	506430	511553	503632	507189	no_	light
	608	756	954	4470	9436	4997	4109	1109	light	
	52	135	103	1045	2048	1364	582	25	mor	e_
September	527103	526881	517016	515170	513351	514759	516131	517336	no_	light
	401	550	816	2264	3934	2860	1699	576	light	
	1	74	82	480	629	295	84	2	mor	e_